16th European Signal Processing Conference (EUSIPCO 2008), Lausanne, Switzerland, August 25-29, 2008, copyright by EURASIP

BLIND SEPARATION OF SECONDARY RADAR SIGNALS USING TIME-FREQUENCY ANALYSIS

M. Tria† *and M. Benidir*† *and E. Chaumette*‡

† L.S.S. (UMR 8506), Supelec, 91192 Gif-sur-Yvette cedex, France

‡ ONERA, DEMR, BP 72, 92322 Chatillon, France

email : {tria,benidir}@lss.supelec.fr, chaumette@onera.fr

ABSTRACT

In Secondary Surveillance Radar (SSR) systems, it is more difficult to locate and recognise aircrafts in the neighbourhood of civil airports since aerial traffic becomes greater. Here, we propose to apply a recent Blind Source Separation (BSS) algorithm based on Time-Frequency Analysis, in order to separate messages sent by different aircrafts and falling in the same radar beam in reception. The above source separation method involves joint-diagonalization of a set of smoothed version of spatial Wigner-Ville distributions. The technique makes use of the difference in the $t-f$ signatures of the nonstationary sources to be separated. Consequently, as the SSR sources emit different messages at different frequencies, the above method is fitted to this new application. We applied the technique in simulation to separate SSR replies. Results are provided at the end of the paper.

Keywords : Blind Source Separation, Time-Frequency Analysis, Secondary Radar.

1. INTRODUCTION

Air traffic control consists mainly in detecting aircrafts, identifying them, and estimating their location and speed. This task is made more and more difficult because of greater aerial traffic. In particular, the probability that two aeroplanes fall in the same radar beam of a civil airport is no longer negligible [1, 2]. The radar antenna interrogates aircrafts that return the requested information (i.e. the reply) to the radar antenna. Due to the increase of air traffic, the density of replies increases as well. It is proposed in this paper to separate the replies from two or more airplanes arriving at the same time on the antenna. Since SSR sources emit different messages at different frequencies, we propose to use a recent blind source separation technique based on time-frequency analysis making use of the difference in the $t-f$ signatures of the nonstationary sources to be separated [3, 4].

The paper is organized as follows. In Section 2, we briefly describe the principe and the SSR data model. The theoretical issues of the time-frequency-based Blind Souce Separation (BSS) technique and its practical implementation are recalled in Section 3. Finally, Section 4 proposes some simulation results of SSR signals separation.

2. SECONDARY RADAR

2.1 Principle

The aim of a secondary radar is to receive information from aircrafts in order to locate and recognise them. Aircrafts are equipped with a device called a 'transponder'. An interrogation message is sent to aircrafts. In the past with SSR mode A/C, all aircrafts in the radar range were thus questioned and they answered only in the case they were in the main beam of the secondary radar. Now with the new technology called SSR mode S (where 'S' stands for selectivity), the radar is able to question a limited number of aircrafts so that reducing the density of replies. This technology was designed to reduce the "Garbling" problem resulting from the interference of the replies of two or more airplanes arriving at the same time on the reception antenna [2]. The answer of the transponder is composed of a preamble and a 56 or 112- bits binary message (see figure 1). This message carries the information (altitude, speed, etc.).

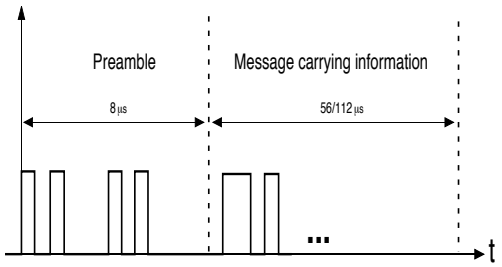

Figure 1: Message to be sent by an aircraft

2.2 Data model

2.2.1 The emitted replies

Let $b(t)$ the message emitted by the transponder and represented in figure 1. Before being emitted, the message is up-converted to the frequency band $f = [f_c - B/2, f_c + B/2]$ where f_c is the nominal carrier frequency ($f_c =$ 1093 MHz), B is the bandwidth ($B = 6$ MHz) [1, 2]. The resulting signal takes the following form:

$$s(t) = b(t)\cos(2\pi f t) \tag{1}$$

2.2.2 Received data model

We now present complex model for the received signal after downconversion by f_c to baseband [5]. The construction

of the general model is valid under some assumptions: the model is based on *narrow-band* and *far-field* assumptions. Moreover, at reception we consider that during a time interval of interest there are M single-path replies impinging on a N-element Uniform Linear Array (ULA): see [5, 6, 2] for more details.

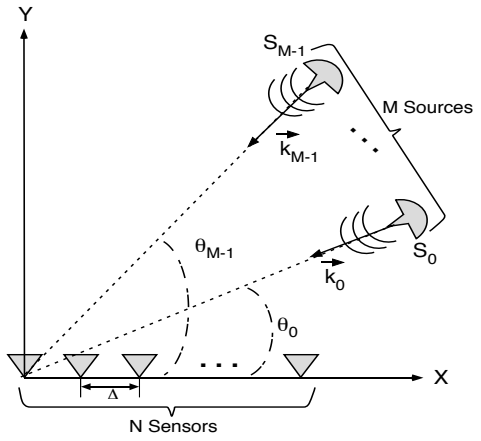

Figure 2: Uniform Linear Array in 2-D geometry.

First for clarity sake, let us considering M sources impinging on only one sensor, the complex model for data recorded by this given sensor is expressed as:

$$d(t) = \sum_{m=0}^{M-1} g(\theta_m) \exp(-j\vec{k_m} \cdot \vec{r}) s_m(t) + \eta(t) \qquad (2)$$

where $g(\theta)$ is the response of the sensor that depends on the direction of propagation θ (defined counter-clockwise relative the X-axis) of the emitted signal (the response is assumed to be flat over the signal bandwidth), $\vec{r} = (x,y)^T$ is the position vector of the sensor, $\vec{k_m} = k\big(\cos\theta_m, \sin\theta_m\big)^T$ is the wavevector of the source with index m noted $s_m(t)$ with $k = 2\pi f/c$ (f: frequency, c: speed of propagation) and θ_m is the direction of propagation of the source with index m. $\eta(t)$ refers to noise. The sources $\{s_m(t)\}_{0 \leqslant m \leqslant M-1}$ in (2) are obtained from the emitted signals in the form of (1) by downconversion by f_c to baseband, including an Hilbert filtering stage.

Now we give the general model by considering the 2-D geometry in the figure 2, i.e. we suppose that M sources impinge on an N-element antenna array of ULA geometry ($N > M$), from distinct DOAs (Direction Of Arrival) $\theta_0, ..., \theta_{M-1}$. Moreover we assume that all the sensors have the same directivity $g_0(\theta) = ... = g_{N-1}(\theta) = g(\theta)$. Consequently the array output vector is obtained as :

$$\mathbf{d}(t) = \mathbf{A}\mathbf{s}(t) + \eta(t) \qquad (3)$$

where $\mathbf{d}(t) = [d_0(t) \cdots d_{N-1}(t)]^T$ are the data collected by the N sensors, $\mathbf{A}$ is a mixing matrix ($N \times M$) , $\mathbf{s}(t) = [s_0(t) \cdots s_{M-1}(t)]^T$ denote the M baseband sources, $\eta(t) = [\eta_0(t) \cdots \eta_{N-1}(t)]^T$ is the noise vector. By recalling that in ULA geometry, the location of the sensor with index n is $\vec{r_n} = \big(n\Delta\ ,\ 0\big)^T$, the elements of the matrix $\mathbf{A}$ are:

$$\{A_{n,m}\}_{\substack{0 \leqslant n \leqslant N-1 \\ 0 \leqslant m \leqslant M-1}} = g(\theta_m) \exp\big(-jkn\Delta\cos\theta_m\big) \qquad (4)$$

where Δ is the distance between two consecutive sensors (see figure 2) such that $\Delta \leqslant \lambda/2$ where $\lambda = c/f$ is the wavelength.

Each transponder do not exactly emit at the nominal carrier frequency f_c but at a frequency $f = f_c + \delta$ where δ is a deviation relative to the nominal frequency. This deviation is proper to each transponder. In other words, the sources emit theirs messages at different frequencies. Now let us make two assumptions concerning the sources and the noise. These assumptions will be used in the time-frequency-based blind source separation algorithm described next. These assumptions are the following ones:

H1) Since transponders generally emit different messages at different frequencies, it can be reasonably assumed that the sources $\{s_m\}_{0 \leqslant m \leqslant M-1}$ are mutually uncorrelated [1].

H2) As the noise mainly originates from the thermal noise of the receiver, but also from atmospheric sources, we assume that the noise vector is spatially white, and that its entries $\{\eta_0(t), ..., \eta_{N-1}(t)\}$ are Gaussian, independent identically distributed (i.i.d) with equal variance σ^2 [2].

3. TIME-FREQUENCY-BASED BLIND SOURCE SEPARATION

3.1 Principle

The problem of Blind Source Separation (BSS) in its simplest form consists in recovering N mutual independent unknown sources from the sole observations of M instantaneous linear mixtures of these sources. Belouchrani and Amin (1998) proposed a method for blind separation of nonstationary sources in the overdetermined case ($M \geqslant N$) [3]. This method relies on joint-diagonalization of a set of spatial time-frequency distributions (STFDs) of the whitened observations at selected time-frequency (t-f) locations. Févotte and Doncarli (2004) extended the BSS technique to the stochastic case and proposed a new criterion that allows to select more efficiently the time-frequency locations where the spatial matrices should be joint-diagonalized [4]: this is this algorithm that we use for recovering the SSR replies.

3.2 Theoretical background

In this paragraph, we revisit the main equations of the BSS technique developed in [3, 4]. We consider the same model as (3):

$$\mathbf{d}(t) = \mathbf{A}\mathbf{s}(t) + \eta(t) \qquad (5)$$

where $\mathbf{d}(t) = [d_0(t) \cdots d_{N-1}(t)]^T$ is the vector of size N containing the observations, $\mathbf{s}(t) = [s_0(t) \cdots s_{M-1}(t)]^T$ is the vector of size M containing the sources supposed nonstationary, zero-mean and mutually uncorrelated, $\mathbf{A}$ is the $N \times M$ unknown full-rank mixing matrix (with $N \geqslant M$), and $\eta(\mathbf{t})$ is an independent identically distributed (i.i.d) noise vector, independent of the sources with

$$E\Big\{\eta\left(t+\frac{\tau}{2}\right)\eta^H\left(t-\frac{\tau}{2}\right)\Big\} = \delta(\tau)\sigma^2\mathbf{I}_N \qquad (6)$$

$\mathbf{I}_N$ denotes the identity matrix of size N, $\delta(\tau)$ the Dirac δ function, ^{H} "conjugate transpose", and σ^2 the unknown variance of the noise, assumed identical for all observations.

The overall objective of BSS is to find an estimate $\hat{A}$ of A, up to the standard BSS indeterminacies on ordering and scale. Once $\hat{A}$ is known, the sources are estimated by:

$$\hat{\mathbf{s}}(t) \stackrel{def}{=} \hat{A}^{\#}\mathbf{d}(t) \approx C\mathbf{s}(t) + \hat{A}^{\#}\eta(t) \tag{7}$$

where $^{\#}$ denotes the Moore-Penrose pseudoinverse and C is a permutation matrix.

3.2.1 From Time-lag to Time-Frequency Plane

Using the sources uncorrelation assumption at time t and lag τ, the covariance of $\mathbf{s}(t) = [s_0(t), ..., s_{M-1}(t)]^T$ is written as:

$$\begin{aligned} \mathscr{R}_{\mathbf{ss}}(t,\tau) &\stackrel{def}{=} E\left\{\mathbf{s}\left(t+\frac{\tau}{2}\right)\mathbf{s}^H\left(t-\frac{\tau}{2}\right)\right\} &(8)\\ &= \mathrm{diag}[\rho_0(t,\tau), ..., \rho_{M-1}(t,\tau)] &(9)\end{aligned}$$

where for fixed values (t,τ), $\mathrm{diag}[\rho_0(t,\tau), ..., \rho_{M-1}(t,\tau)]$ is a diagonal matrix whose diagonal elements starting in the upper left corner are $\rho_0(t,\tau), ..., \rho_{M-1}(t,\tau)$; with $\rho_m(t,\tau) \stackrel{def}{=} E\left\{s_m\left(t+\frac{\tau}{2}\right)s_m^*\left(t-\frac{\tau}{2}\right)\right\}$, $m = 0, ..., M-1$, where * denotes complex conjugate.

Now using (5), the covariance matrix $\mathscr{R}_{\mathbf{dd}}(t,\tau)$ of $\mathbf{d}$(t) is:

$$\mathscr{R}_{\mathbf{dd}}(t,\tau) = \mathbf{A}\mathscr{R}_{\mathbf{ss}}(t,\tau)\mathbf{A}^H + \delta(\tau)\sigma^2\mathbf{I}_N \tag{10}$$

From (10), the Spatial Wigner-Ville Spectrum (SWVS) is obtained by Fourier transform of $\mathscr{R}_{\mathbf{dd}}(t,\tau)$ with respect to τ:

$$\overline{\mathscr{W}}_{\mathbf{dd}}(t,f) \stackrel{def}{=} \int_{-\infty}^{+\infty} \mathscr{R}_{\mathbf{dd}}(t,\tau)e^{-j2\pi f\tau}d\tau \tag{11}$$

For a given $t-f$ location (t_i, f_j), $\overline{\mathscr{W}}_{\mathbf{dd}}(t_i,f_j)$ is a square matrix of size N which diagonal elements contain the auto Wigner-Ville spectra (WVS) of the observations at $(t,f) = (t_i,f_i)$, whereas nondiagonal elements contain cross-WVS at $(t,f) = (t_i,f_j)$. In the $t-f$ plane, (10) becomes:

$$\overline{\mathscr{W}}_{\mathbf{dd}}(t,f) = \mathbf{A}diag\left[\overline{\omega}_o(t,f), ..., \overline{\omega}_{M-1}(t,f)\right]\mathbf{A}^H + \sigma^2\mathbf{I}_N \tag{12}$$

with $\overline{\omega}_m(t,f)$ the Fourier transform of $\rho_m(t,\tau)$ with respect to τ; $m = 0, ..., M-1$.

One can write eq. (12) as:

$$\overline{\mathscr{W}}_{\mathbf{dd}}(t,f) = \mathbf{A}\overline{\mathscr{W}}_{\mathbf{ss}}(t,f)\mathbf{A}^H + \sigma^2\mathbf{I}_N \tag{13}$$

where $\overline{\mathscr{W}}_{\mathbf{ss}}(t,f) = diag\left[\overline{\omega}_o(t,f), ..., \overline{\omega}_{M-1}(t,f)\right]$.

3.2.2 Recovering of matrix A

The first step consists in turning the recovering of the $N \times M$ mixing matrix $\mathbf{A}$ into the determination of a $M \times M$ unitary matrix $\mathbf{U}$. Let $\mathbf{W}$ be an $M \times N$ full-rank matrix such that $\mathbf{W}(\mathbf{A}\mathbf{A}^H)\mathbf{W}^H = \mathbf{I}_M$. Actually, the matrix $\mathbf{W}$ allows the whitening of the noise-compensated observations $\mathbf{y}(t) = \mathbf{d}(t) - \eta(t) = \mathbf{A}\mathbf{s}(t)$. Indeed, let us consider the signals $\mathbf{z}(t) = \mathbf{W}\mathbf{y}(t)$, we have:

$$E\left\{\mathbf{z}(t)\mathbf{z}^H(t)\right\} = \mathbf{W}\mathbf{A}E\left\{\mathbf{s}(t)\mathbf{s}^H(t)\right\}\mathbf{A}^H\mathbf{W}^H \tag{14}$$

With the source decorrelation assumption and assuming the source signals with unit power, we have $E\left\{\mathbf{s}(t)\mathbf{s}^H(t)\right\} = \mathbf{I}_M$. Consequently eq.(14) becomes:

$$E\left\{\mathbf{z}(t)\mathbf{z}^H(t)\right\} = \mathbf{W}\mathbf{A}\mathbf{A}^H\mathbf{W}^H = \mathbf{I}_M \tag{15}$$

and the signals $\mathbf{z}(t)$ are the whitened noise-compensated observations and $\mathbf{W}$ is called a "whitening" matrix.

Let $\mathbf{U} = \mathbf{W}\mathbf{A}$. From the definition of $\mathbf{W}$, $\mathbf{U}$ is unitary, and $\mathbf{A}$ satisfies:

$$\mathbf{A} = \mathbf{W}^{\#}\mathbf{U}. \tag{16}$$

In this paragraph, we suppose that $\mathbf{W}$ and the noise variance σ^2 are known (we will see in the next paragraph that they can be estimated from the correlation matrix of the observations). From now, our objective is to determine $\mathbf{U}$ with the knowledge of $\overline{\mathscr{W}}_{\mathbf{dd}}(t,f)$, $\mathbf{W}$ and σ^2. By following the steps in Section 3.2.1 with $\mathbf{z}(t) = \mathbf{W}(\mathbf{d}(t) - \eta(t))$, we can define "whitened and noise-compensated" SWVS-matrices $\overline{\mathscr{W}}_{\mathbf{zz}}(t,f)$ [4] that expresses as:

$$\overline{\mathscr{W}}_{\mathbf{zz}}(t,f) = W\left(\overline{\mathscr{W}}_{\mathbf{dd}}(t,f) - \sigma^2\mathbf{I}_N\right)W^H \tag{17}$$

Combining eq. (13) and eq. (17), we have:

$$\overline{\mathscr{W}}_{\mathbf{zz}}(t,f) = U\overline{\mathscr{W}}_{\mathbf{ss}}(t,f)U^H \tag{18}$$

Since $\overline{\mathscr{W}}_{\mathbf{ss}}(t,f)$ is diagonal for any (t,f) and since $\mathbf{U}$ is unitary, $\mathbf{U}$ diagonalizes $\overline{\mathscr{W}}_{\mathbf{zz}}(t,f)$ for any (t,f). Consequently, $\mathbf{U}$ may be obtained as a unitary matrix diagonalizing any "whitened and noise-compensated" matrix $\overline{\mathscr{W}}_{\mathbf{zz}}(t,f)$. The mixing matrix $\mathbf{A}$ is then computed with eq. (16) and the sources are retrieved with (7).

3.3 The method in practice

Now we consider the practical implementation of the above method. This implementation was proposed by Fevotte and Doncarli [4]. Because only one realization of the observations is generally available, we have to estimate the Wigner-Ville Spectrum (WVS). It is shown in [7, 8] that a smoothed version of the Wigner-Ville Distribution (WVD) is a good estimate of the WVS. For a given smoothing kernel $\phi(t,f)$ we denote $\mathscr{W}^{\phi}(t,f)$ the smoothed version of the WVD $\mathscr{W}(t,f)$:

$$\mathscr{W}^{\phi}_{\mathbf{dd}}(t,f) \stackrel{def}{=} \int_{-\infty}^{+\infty}\int_{-\infty}^{+\infty} \phi(u-t, v-f)\mathscr{W}_{\mathbf{dd}}(u,v)dudv \tag{19}$$

where $\mathscr{W}_{\mathbf{dd}}(t,f)$ is defined as:

$$\mathscr{W}_{\mathbf{dd}}(t,f) \stackrel{def}{=} \int_{-\infty}^{+\infty} \mathbf{d}\left(t+\frac{\tau}{2}\right)\mathbf{d}^H\left(t-\frac{\tau}{2}\right)e^{-j2\pi f\tau}d\tau \tag{20}$$

Using the estimate $\mathscr{W}^{\phi}_{\mathbf{dd}}(t,f)$ of $\overline{\mathscr{W}_{\mathbf{dd}}}(t,f)$, eq.(18) becomes:

$$\mathscr{W}^{\phi}_{\mathbf{zz}}(t,f) \approx U\mathscr{W}^{\phi}_{\mathbf{ss}}(t,f)U^H \tag{21}$$

where

$$\mathscr{W}^{\phi}_{\mathbf{zz}}(t,f) \stackrel{def}{=} \hat{W}\left(\mathscr{W}^{\phi}_{\mathbf{dd}}(t,f) - \hat{\sigma}^2\mathbf{I}_m\right)\hat{W}^H \tag{22}$$

where $\hat{W}$ and $\hat{\sigma}^2$ are the estimates of W and σ^2 obtained classically from the eigenelements of the empirical correlation matrix of the observations [3, 9].

At this step, $\mathscr{W}_{\mathbf{zz}}^{\phi}(t,f)$ is known. Now, we have to estimate U from (21). $\mathscr{W}_{\mathbf{ss}}^{\phi}(t,f)$ is only an estimate of $\overline{\mathscr{W}}_{\mathbf{ss}}(t,f)$ and it is not diagonal for every $t-f$ location (as opposed to $\overline{\mathscr{W}}_{\mathbf{ss}}(t,f)$; see 3.2.1). Bélouchrani and Amin proposed to estimate U throught *joint-diagonalization* of a set of K matrices $\{\mathscr{W}_{\mathbf{zz}}^{\phi}(t_i,f_i)\}$ at K $t-f$ locations $\{(t_i,f_i); i = 1...,K\}$ for which $\mathscr{W}_{\mathbf{ss}}^{\phi}(t_i,f_i)$ is diagonal [3]. The above authors noticed that searching the above set of $t-f$ locations is equivalent to detect "single autoterm" locations. Févotte and Doncarli proposed a new criterion that allows a more efficient selection of the time-frequency locations [4] (see also [12] for a more recent criterion). The overall Time-Frequency-based Blind Source Separation (TFBSS) algorithm can be found in [10]. Once an estimate $\hat{U}$ is available, an estimation of the mixing matrix A is then obtained as follows:

$$\hat{A} = \hat{W}^{\#}\hat{U} \tag{23}$$

and the sources are retrieved with (7).

4. SIMULATION RESULTS

Here we consider three sensors and two sources. The distance between 2 sensors is fixed to $\Delta = 12$ cm in order that $\Delta \leqslant c/(2f_c)$ where $f_c = 1093$Mhz and $c = 3\times 10^8$m/s are the central carrier frequency and the propagation speed of the signals respectively. The 2 sources S_1 and S_2 emit different messages $b_1(t)$ and $b_2(t)$ whose carrier frequencies are $f_1 = 0.7$MHz and $f_2 = 1$MHz respectively after down-conversion by f_c to baseband. The 2 sources emit at the direction of propagation $\theta_1 = \pi/6$ (in radians) and $\theta_2 = \pi/4$ (in radians) respectively. We choose the response of the sensors equal to unity at $\theta = \theta_0$ and $\theta = \theta_1$, i.e. $g(\theta_0) = g(\theta_1) = 1$. We applied the TFBSS to the real-valued data corresponding to model in equation eq. (3):

$$\mathbf{d}(t) = \mathbf{A}\mathbf{s}(t) + \eta(t) \tag{24}$$

where $\mathbf{d}(t) = [d_0(t)\, d_1(t)\, d_2(t)]^T$ and $\mathbf{s}(t) = [s_0(t)\, s_1(t)]^T$ are the 3 observations and the 2 baseband sources respectively. The elements of the matrix $\mathbf{A}$ are computed as:

$$\{A_{n,m}\}_{\substack{0\leqslant n\leqslant 2\\ 0\leqslant m\leqslant 1}} = g(\theta_m)\cos\left(k_c n\Delta\cos\theta_m\right) \tag{25}$$

where $k_c = 2\pi f_c/c$. We simulated zero-mean White Gaussian noises $\{\eta_n(t)\}_{0\leqslant n\leqslant 2}$ with same variance $\sigma^2 = 3\times 10^{-2}$.

Figure 3 shows the two messages in the form of the figure 1. These messages are provided by the sources (transponders). Before being emitted by the sources, they are up-converted to the frequency band (see section 2.2.1). The messages are chosen uncorrelated as we can see in figure 3. In this paper we choose the Smoothed Pseudo Wigner-Ville Distribution [11] as the smoothed version of the WVD in (19). In this paper we do not study the choice of the smoothing kernel in eq. (19). Figure 4 represents the Time-Frequency Representation of the baseband signals emitted by the sources. We can see that the signals are located at the two different carrier frequencies we chose for the signals, i.e. $f_1 = 0.7$MHz and $f_2 = 1$MHz respectively. By observing the distribution along the time axis, clearly the signals are nonstationary relative to time. Figure 5 shows the three observations recorded by the sensors. They are obtained by following the model (24). Figure 6 shows the estimated sources $\hat{s}_0(t)$ and $\hat{s}_1(t)$ (after fixing permutation, sign and scale) obtained from the above data. The previous estimates are compared with the corresponding theoretical sources $s_0(t)$ and $s_1(t)$. In order to match the estimated sources with the original ones, we compute the cross-correlation between original and estimated sources:

$$C_i = \frac{\int s_i(t)\hat{s}_i(t)dt}{E_i}\ ;\ i = \{0,1\} \tag{26}$$

where $E_i = \int s_i(t)s_i(t)dt$ is the energy of the source $s_i(t)$, used for normalisation. With the definition (26), the cross-correlation is close to unity if the estimate is close to the original source. We have $C_0 = 0.9995$ for the first source, and $C_1 = 0.9996$ for the second source. With the above results and by observing Figure 6, we conclude that the separation of the signals is of satisfactory quality. After the separation is completed by the TFBSS algorithm, postprocessing is performed on each channel output to recover the codes presented in Figure 3.

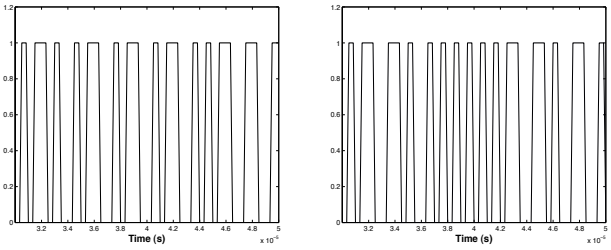

Figure 3: Portion of the messages (codes) to be sent by the first source (left) and the second source (right).

5. CONCLUSION AND PERSPECTIVES

The simulation example that we propose in this paper with realistics parameters, reveals that the Secondary Radar sources can be recovered almost perfectly using the TFBSS algorithm. Consequently the technique seem very promising for the real-world problem. The robustness of the TFBSS technique is due to the use of the decorrelation, the nonstationarity and the $t-f$ localization differences of the signals to be separated. In a further theoretical work we could address the problem of searching the optimal smoothing kernels since it was demonstrated in [3] that the choice of the $t-f$ kernel has a direct impact on the performance of the TFBSS.

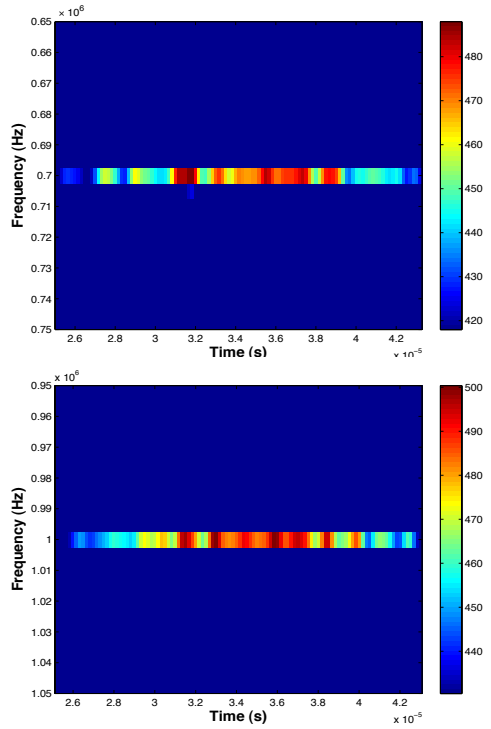

Figure 4: Time-Frequency signatures of the baseband signals emitted by the first source (above) and the second source (below).

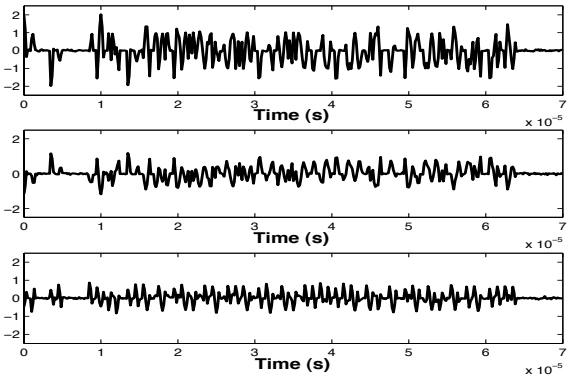

Figure 5: Observations collected by the first sensor (above), the second sensor (middle), the third sensor (below).

REFERENCES

[1] E. Chaumette, P. Comon and D. Muller, ICA-based technique for radiating sources estimation: application to airport surveillance, *IEE Proc. F. Radar Signal Processing*, **140**(6), pp. 395-401.

[2] N.L.R. Petrochilos, *Algorithms for Separation of Secondary Surveillance Radar Replies*, Ph. Doctorate, University of Nice (France, 2002).

[3] A. Belouchrani and M.G. Amin, Blind Source Separation Based on Time-Frequency Signal Representations, *IEEE Trans. on Signal Processing*, **46** (Nov. 1998), pp. 2888-2897.

[4] C. Févotte and C. Doncarli, Two contributions to Blind Source Separation Using Time-Frequency Distributions, *IEEE Signal Processing Letters*, **11** (March. 2004), pp. 386-389.

[5] H. Krim and M. Viberg, Two decades of array signal processing research, *IEEE Sig. Proc. Magazine* (July 1996), pp. 67-94.

[6] S. Haykins, *Radar Array Processing*, Springer-Verlag, 1993.

[7] W. Martin and P. Flandrin, Wigner-Ville spectral analysis of nonstationary processes, *IEEE Trans. Acoust., Speech, Signal Processing*, **ASSP-33** (Dec. 1985), pp. 1461-1470.

[8] A.M. Sayeed and D.L. Jones, Optimal kernels for non-stationary spectral estimation, *IEEE Trans. Signal Processing*, **43** (Feb. 1995), pp. 478-491.

[9] A. Belouchrani and K. Abed-Meraim and J-F Cardoso and E. Moulines, A Blind Source Separation Technique Based on Second Order Statistics, *IEEE Trans. on Signal Processing*, **45** (Feb. 1997), pp. 434-444.

[10] C. Févotte, *Approche temps-fréquence pour la séparation aveugle de sources non-stationnaires*, Ph. Doctorate, University of Nantes (France, 2003).

[11] P. Flandrin, *Temps-fréquence*, Hermés (1998), Paris.

[12] L. Giulieri, N. Thirion-Moreau, and P. Y. Arques, Blind source separation using bilinear and quadratic time-frequency representations, *Proceedings of ICA*, 2001.

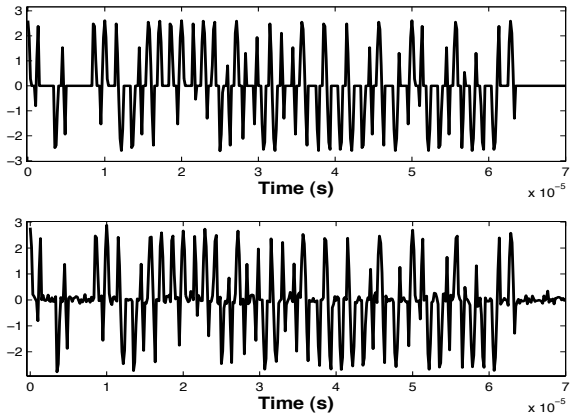

(a) First original source (above) and its estimate (below).

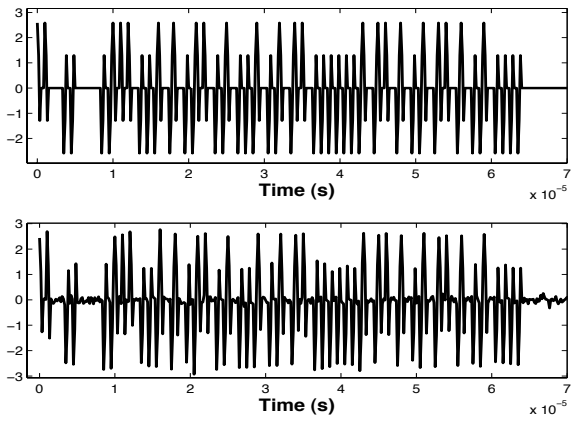

(b) Second original source (above) and its estimate (below).

Figure 6: Comparison of the original sources with theirs estimates.